

Earth ArXiv

This is a non-peer-reviewed preprint submitted to EarthArXiv.

This manuscript has been submitted for publication in Tunnelling and Underground Space Technology. Please note the manuscript has yet to be formally accepted for publication. Subsequent versions of this manuscript may have slightly different content. If accepted, the final version of this manuscript will be available via the 'Peer-reviewed Publication DOI' link on the right-hand side of this webpage. Please feel free to contact any of the authors; we welcome feedback.

1 Managing Squeezing Rock Mass with TBM 2 Data Analysis: Rail Link Rishikesh – 3 Karnaprayag (India)

4 Georg H. Erharter¹, Sumit Jain², Øyvind Dammyr¹, Sjur Beyer^{1*},
5 Rajinder K. Bhasin¹

6 1) Norwegian Geotechnical Institute, Oslo, Norway

7 2) Rail Vikas Nigam Limited (RVNL), New Delhi, India

8 * correspondence: sjur.beyer@ngi.no

9 **Preprint statement:** *This manuscript is a non-peer reviewed preprint submitted to EarthArXiv.*

10 Abstract

11 The 125.2 km rail link Rishikesh–Karnaprayag in the Lesser Himalayas of India represents a
12 benchmark in mechanized tunnelling through complex geology. This paper focuses on Tunnel 8,
13 a 14.58 km section excavated primarily using two single-shield hard rock tunnel boring machines
14 (TBM) under challenging conditions characterized by tectonically deformed, partly water-bearing
15 phyllites and high in-situ stresses, thus squeezing rock mass conditions were at hand. Both TBMs
16 were equipped with advanced instrumentation, including a Void Measuring System (VMS) for
17 real-time monitoring of shield gap size and tunnel wall deformation rates that was used
18 consistently throughout the whole tunnel. The collected shield gap data constitutes one of the
19 rare cases of continuous tunnel wall deformation rates in shielded TBM excavation. An integrated,
20 near-real-time data analysis framework was developed to continuously assess TBM operational
21 parameters, enabling proactive control and optimization of excavation performance. Within that
22 framework, the VMS data was used to run a novel analytical model-based squeezing risk
23 monitoring system integrating gross TBM advance speed, tunnel wall deformation rate, shield
24 length, and shield gap size. Additionally, tunnel seismic prediction was employed to characterize
25 geology ahead of the face, and supervised machine learning algorithms were implemented for
26 rapid interpretation and visualization, facilitating informed decision-making by TBM operators.
27 The project demonstrates how advanced monitoring systems and data-driven tunnelling can
28 significantly enhance TBM performance and risk management in geotechnically adverse
29 conditions. Key operational insights and recommendations are provided to guide future TBM
30 projects in similar geological environments.

31 **Keywords:** TBM Excavation, Squeezing Ground, Hard Rock, Data Analysis, Machine Learning

32 Highlights

- 33 ▪ Data-centric tunnelling optimized TBM performance in complex Himalayan geology.
- 34 ▪ Unprecedented analysis of shield gap monitoring in hard rock TBM excavation.
- 35 ▪ Analytical model developed to permanently monitor squeezing risk during excavation.

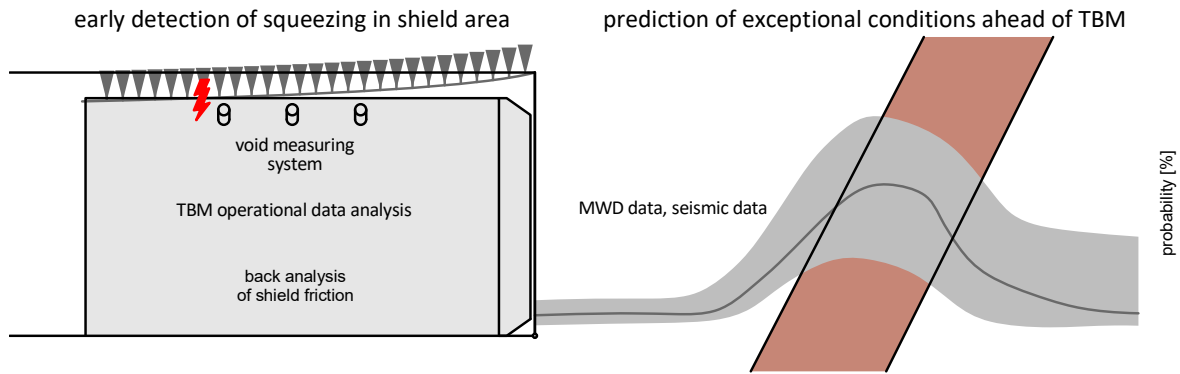
- 36 ▪ Seismics and machine learning used to predict excavation conditions ahead of face.

37 1. Introduction

38 Tunnel boring machines (TBM) have become the excavation method of choice for long tunnels (>
39 2km) in mostly homogeneous hard rock ground conditions (Maidl et al., 2008; Maidl et al., 2013;
40 Bobet and Einstein, 2024). One significant challenge that can occur is squeezing rock mass,
41 which poses threats ranging from reduced excavation performance to downtimes of several
42 months if a TBM gets fully stuck (Barla, 2001; Ramoni and Anagnostou, 2010, 2011). According to
43 Barla (2001) (see therein for earlier references) squeezing “stands for large time-dependent
44 convergence during tunnel excavation. It takes place when a particular combination of induced
45 stresses and material properties pushes some zones around the tunnel beyond the limiting shear
46 stress at which creep starts. Deformation may terminate during construction or continue over a
47 long period of time.” Conventionally, squeezing is dealt with by special measures like shield
48 lubrication which may or may not work well (Erharter et al., 2023). Alternatively the TBM operation
49 can be adapted to avoid problems with squeezing which means maintaining a minimum gross
50 advance speed and avoiding longer foreseeable stops (e.g. cutterhead- or conveyor belt
51 maintenance) in areas of squeezing rock mass conditions. Especially when this strategy is
52 followed, availability of comprehensive information about the state of the TBM excavation is key
53 to overcoming challenging ground conditions.

54 While on-site observations remain a major source of that information, modern TBMs are
55 equipped with hundreds of sensors that continuously record a wealth of data - the TBM
56 operational data. TBM operational data comprehensively represents the system behavior of an
57 ongoing TBM excavation (i.e. the interaction of the TBM with the rock mass (Erharter et al., 2025b;
58 Erharter, 2026)) as it is the product of three main influences: the rock mass, the TBM machinery
59 and the way the TBM is operated. Consequently, TBM operational data can be used as a main
60 source of information for TBM excavation and system behavior monitoring.

61 This contribution focuses on using TBM operational data to overcome challenging ground
62 conditions and presents results from the case study of the Rishikesh-Karnaprayag project (India)
63 where squeezing rock mass conditions of the lesser Himalayas were tackled with two single
64 shield TBMs. While general state-of-the-art TBM operational data monitoring was conducted for
65 this project (Erharter et al., 2025b), the Rishikesh-Karnaprayag project went beyond that by i)
66 developing and implementing a data-driven methodology for early detection of squeezing in the
67 shield area of a TBM and ii) developing a machine learning (ML)-based method to predict
68 exceptional advance conditions ahead of the TBM. The two goals are illustrated in Figure 1.



69

70 *Figure 1: Schematic of the two data-driven development goals for the Rishikesh-Karnaprayag project. Left: an early*
71 *detection system for squeezing in the shield area, right: a system to predict exceptional conditions ahead of the TBM.*

72 Both development goals were intended as decision support and early warning tools for onsite
73 personnel. It should also be emphasized that the development was done while the project was
74 executed and not in retrospective. Consequently, the development had to be flexible and to some
75 degree pragmatic as the excavation conditions and the available data continuously developed
76 and changed. This needs to be considered in contrast with other academic works in the context
77 of digitalization, data-centric tunneling and ML in geotechnical engineering which are often
78 conducted on static, final or simulated datasets (Erharter and Marcher, 2020; Hansen et al.,
79 2024a; Hansen et al., 2024b), without an imminent pressure to deliver monitoring results and
80 predictions. While development pressure incentivizes efficient solutions, it also diminishes the
81 degree to which comprehensive sensitivity analyses can be done. Nevertheless, the data analysis
82 development work that was conducted at the Rishikesh-Karnaprayag project is a valuable case
83 study as it pushed the boundaries of what can be achieved with TBM operational data monitoring
84 in a practical tunneling project today and thus serves as a role model for future projects in similar
85 conditions.

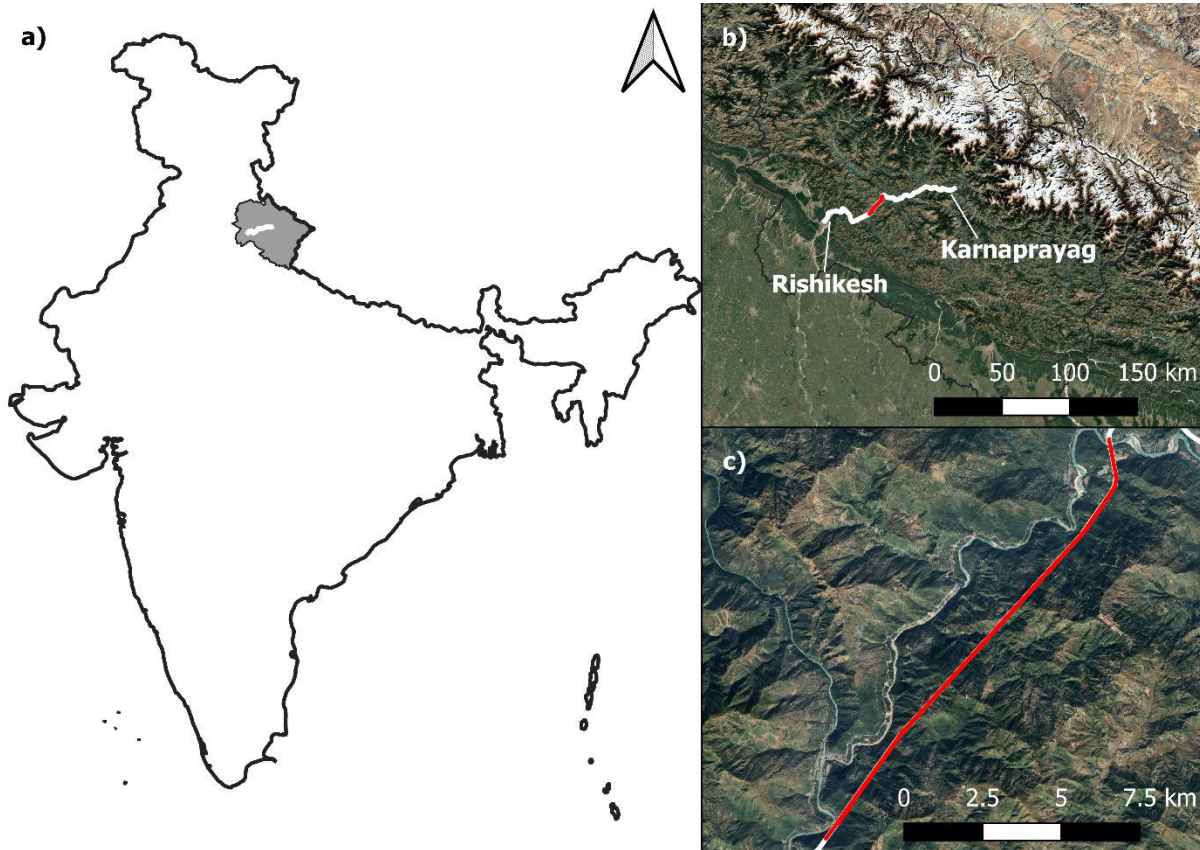
86 Section 2 gives an outline of the project and its geology, information about the deployed TBMs
87 and special sensory systems and a description of the encountered challenging rock mass
88 conditions. Based on these prerequisites, a fully automatic data processing framework was
89 developed together with a new analytical method for predicting squeezing risk for single shield
90 TBMs, as well as a ML-based prediction system that forecasts exceptional advance conditions.
91 These methodological explanations will be given in section 3. Section 4 will show the
92 observations that were made on-site using these methods, which includes one of the first ever
93 reports of a continuous tunnel wall deformation record for a single shield TBM tunnel drive. The
94 TBM operational data-related developments and observations from the Rishikesh-Karnaprayag
95 project will then finally be discussed in section 5 and conclusions and recommendations for
96 future projects are provided in section 6.

97 2. Project Overview and Background

98 2.1. Rail Link Rishikesh – Karnaprayag

99 Rail Vikas Nigam Limited (RVNL), a navratna CPSU under Ministry of Railways, is constructing the
100 125.2 kilometers long Rishikesh-Karnaprayag Railway Project. The route is in the Indian state of

101 Uttarakhand and goes in a north-eastward direction from the existing Virbhadrha Railway Station
 102 near Rishikesh and culminates at the newly designed Karnaprayag Railway Station. The project
 103 comprises 213.45 kilometers of tunnelling, including 16 main tunnels, 13 escape tunnels, 7 adit
 104 tunnels, and numerous cross passages, traversing along the fragile and seismically active
 105 Himalayan belt, following the Ganga and Alaknanda River valleys with rugged topography and
 106 complex geology. This paper reports on developments and observations from “Tunnel 8” of the
 107 project which connects Devprayag Railway Station with Janasu Railway Station through a 14.58
 108 km double line tunnel. An overview map of the whole project and the location of Tunnel 8 is given
 109 in Figure 2.



110

111 *Figure 2: Overview map. a) position of the Rishikesh-Karnaprayag route section (white) within the Indian state of*
 112 *Uttarakhand (grey). b) detail view of the route section within Uttarakhand, tunnel 8 in red. c) detail view onto Tunnel 8*
 113 *along the Alaknanda river.*

114 RVNL awarded the construction work of Tunnel 8 to M/s Larsen and Toubro (contractor). Tunnel 8
 115 comprises two tunnel tubes (termed “Upline” and “Downline”) which were excavated by single
 116 shield TBMs (see next section for technical details). Both TBMs completed their excavations
 117 strictly on schedule (Table 1).

118 *Table 1: Timelines and chainages of both TBMs at the Rishikesh-Karnaprayag project.*

TBM	Boring start (planned / actual)	Boring completion (planned / actual)	Chainage start	Chainage end	Distance (in Kms)
TBM Shakti (S-01309A)	28.12.2022 / 17.12.2022	28.4.2025 / 16.4.2022	48+180	58+649	10.469
TBM Shiv (S- 01310A)	27.2.2023 / 6.3.2023	30.6.2025 / 30.6.2025	0+880	11+168	10.298

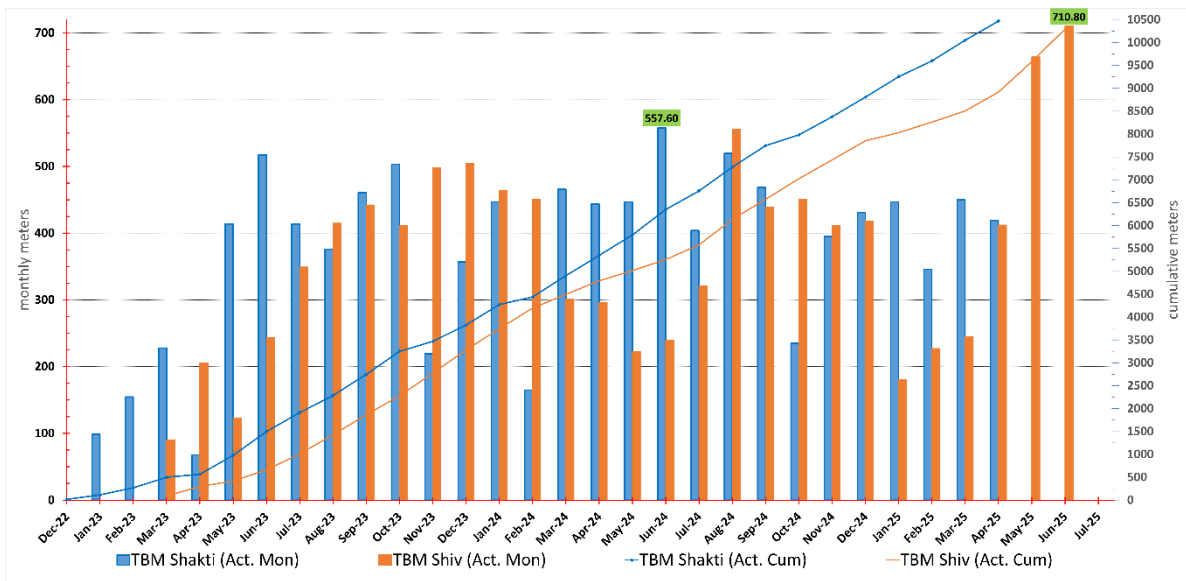
119

120 Both TBMs achieved a high performance with up to 710 meters of excavated tunnel meters in a
 121 month (Table 2). The monthly and cumulative comparison between planned and actual
 122 performance is shown in Figure 3.

123 *Table 2: Monthly time percentage utilization of TBM Shakti and TBM Shiv (excluding initial 3 months learning period).*

Categories	TBM Shakti (S-01309A) Performance			TBM Shiv (S-01310A) Performance		
	Average	Best	Worst	Average	Best	Worst
Excavation	16.47%	21.86%	4.09%	15.48%	26.56%	8.06%
Lining	25.01%	35.21%	7.87%	20.66%	27.86%	9.10%
No Production	58.53%	42.93%	88.4%	63.86%	45.58%	82.84%
Applicable Month	Dec 22 to Apr 25	June 24	Apr 23	Mar 23 to June 25	June 25	Jan 25
Excavated meters per month		557	68		710	182
Applicable Chainage	48+180 to 58+649	53+981 to 54+539	48+679 to 48+747	0+880 to 11+168	10+457 to 11+167	8+726 to 8+908

124



125

126 *Figure 3: Monthly and cumulative excavated tunnel meters for TBM Shakti (S-01309A, Blue) and TBM Shiv (S-01310A,*
 127 *Orange).*

128 Engineering geological investigations for the project were conducted from 2014 to 2018,
 129 progressing from desk studies to detailed field and laboratory investigations. Initial studies
 130 included literature and imagery reviews followed by 2016 field mapping of lithological and
 131 structural features, characterizing rock joints with variable persistence (1–10 m), aperture (0.1–5
 132 mm), and weathering (slight to moderate). In 2018, geotechnical investigations included 15
 133 boreholes (9 along the TBM alignment), geophysical surveys, laboratory testing, and in-situ tests
 134 such as permeability, dilatometer, borehole televiewer, and hydro-fracturing.

135 Tunnel 8 passes through the Lesser Himalayas of the Garhwal region of Uttarakhand. The Lesser
 136 Himalaya includes a thrust-bound sector delineated by two tectonic plates i.e. the Main
 137 Boundary Thrust to the south and the North Almora thrust (NAT). The rock masses present in the

138 area have undergone a complex history of burial and following exhumation, having been
 139 subjected to large stresses with both ductile and brittle deformation representing a fold and
 140 thrust tectonic regime. The geology of Tunnel 8 entirely belongs to low grade metamorphic rocks
 141 of Chandpur formation of Jaunsar Group, having a continuous sequence of light and dark grey
 142 phyllite with interbedded light grey and purple sandstone and siltstone and presence of quartzitic
 143 phyllite. The phyllites are highly crushed and disintegrated because of the NAT. Near the NAT,
 144 these rocks are characterized by slickensides, increased discontinuity density due to crushing,
 145 mylonitization and increased weathering. Rock mass classification using the Rock Mass Rating
 146 (RMR) (Bieniawski, 1973) and the Geological Strength Index (GSI) (Hoek and Brown, 1997) divided
 147 the TBM tunnels into 12 segments, with 74.51% Class III (fair rock), 23.91% Class IV (poor rock),
 148 and 1.58% Class V (very poor rock).

149 2.2. Tunnel Boring Machines and Void Measuring System

150 The two TBMs used at the project are identical Herrenknecht (i.e. TBM manufacturer) hard rock
 151 single shield TBMs with designations "S-01309A" (Shakti) and "S-01310A" (Shiv). The shield
 152 consists of three segments with slightly decreasing diameter (front-, center-, tail-) to achieve an
 153 overall conicity. General technical specifications of the TBMs can be found in Table 3.

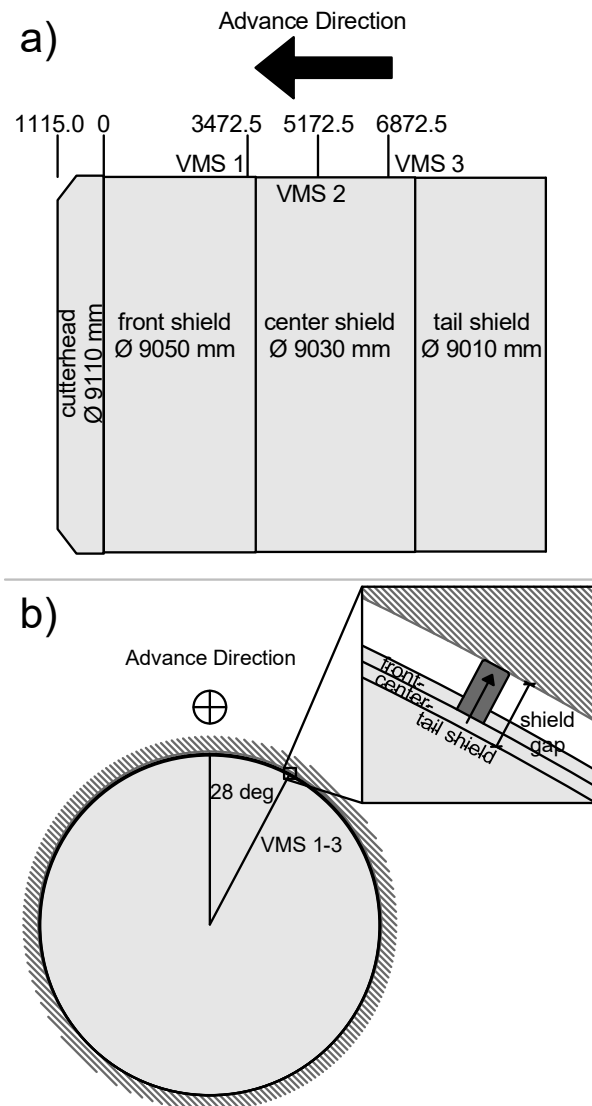
154 *Table 3: Technical specifications of the used single shield TBM.*

Specification	Value
Cutterhead diameter [m]	9.11
Number of cutters	55
Radius of cutters [mm]	241.3
Total shield length [m]	10.68
Shield outer diameters [m]: front / center / tail	9.05, 9.03, 9.01

155
 156 The conicity has the purpose of avoiding that the TBM gets jammed in case a block gets stuck in
 157 the space between the shield and the tunnel wall (i.e. the shield gap) which is typically about 10
 158 to 15 cm at the widest position. A closed shield gap indicates a heavily deformed rock mass or
 159 instabilities in the tunnel wall and can potentially increase the shield friction so much that the
 160 TBM cannot move forward anymore, thus requiring extraordinary measures to free the machine
 161 again. The TBMs are equipped with a Void Measuring System (VMS) which consists of three
 162 radially extendable measuring rods, that can measure the size of this shield gap (Figure 4b). The
 163 single shield TBM of the Frejus Safety Tunnel in the Western Alps is the only other published case
 164 that the authors are aware of where a comparable VMS system was used (Bianchi, 2023).
 165 However, it is not documented that the system was used as consistently, and the data analyzed
 166 as comprehensively as in the Rishikesh-Karnaprayag project.

167 In the Rishikesh-Karnaprayag project, three VMS are installed at 3472.5-, 5172.5- and 6872.5 mm
 168 distance from the leading edge of the front shield (Figure 4a) and they are pointing towards the
 169 tunnel wall at an angle of 28 degrees clockwise from the center of the crown (tunnel roof), seen
 170 in the direction of advance (Figure 4b). The VMS rods have a spacing of 1700 mm in between
 171 them, which corresponds to the length of one stroke of the TBM (ring width = 1700 mm). The
 172 maximum shield gap (maximal rod extension) that can be measured by the VMS is 250 mm. The

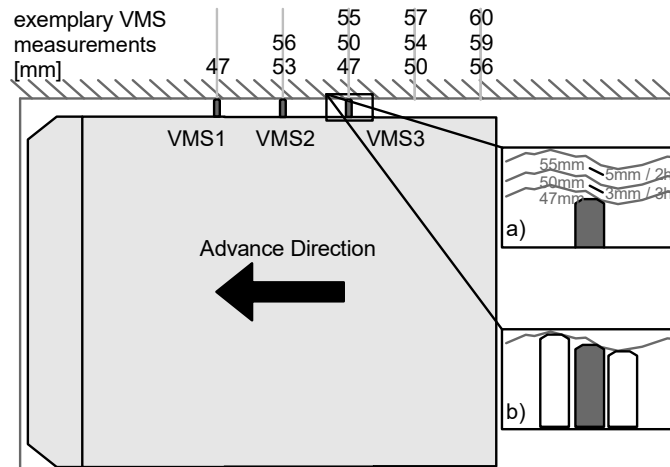
173 VMS system thus indirectly monitors overbreaks from the tunnel wall when the measuring rods
 174 max out.



175
 176 *Figure 4: a) sideview of the TBM geometry and positions of the void measuring system (VMS). b) view in advance*
 177 *direction showing the position of the VMS and a detailed view that shows VMS 3 fully extended.*

178 The VMS data (as all TBM operational data) is inherently time based. When the TBM is in a
 179 standstill position, all VMS take readings, and hence 3 different tunnel chainages with 1700 mm
 180 in between them are measured at the same time. These readings by themselves are valuable, as
 181 they inform about the size of the shield gap on the different positions at the shield. After
 182 subsequent strokes (which ideally are also 1700 mm long), VMS 2 will measure the shield gap in
 183 the previous position of VMS 1 and VMS 3 at the previous position of VMS 2. After three
 184 subsequent strokes, a set of three measurements of the shield gap at the same point is complete.
 185 Given these shield gap measurements and knowing the time between the measurements, the
 186 tunnel wall deformation rate [mm/h] can be computed (Figure 5a). The geometric effect of the
 187 shield conicity (Figure 4a) must be considered and the VMS are sensitive with respect to the TBM
 188 positioning. If the length of the TBM stroke is deviating from 1700 mm, the VMS will not measure
 189 in the same position as before and is thus susceptible to misreadings caused by the tunnel wall

190 roughness (Figure 5b). To reduce the influence of the tunnel wall roughness, only VMS readings
191 were considered where the TBM positioning is within 5 cm of the theoretically correct position
192 (corresponding to the diameter of the tip of the measuring rod).



193

194 *Figure 5: Graphical representation of how tunnel wall deformation rates can be derived from the VMS. a) detailed view*
195 *with exemplary measurements and time differences between TBM advances of 2 and 3 hours respectively. b)*
196 *sensitivity of the VMS to tunnel wall roughness.*

197 2.3. Encountered Ground Conditions

198 Despite all efforts during the planning and construction phases to identify ground conditions to
199 reduce tunnelling risks, discrepancies between actual and predicted conditions were observed
200 in both tubes. These discrepancies included variations in groundwater inflow into the tunnel, and
201 the presence of shear/fault zones.

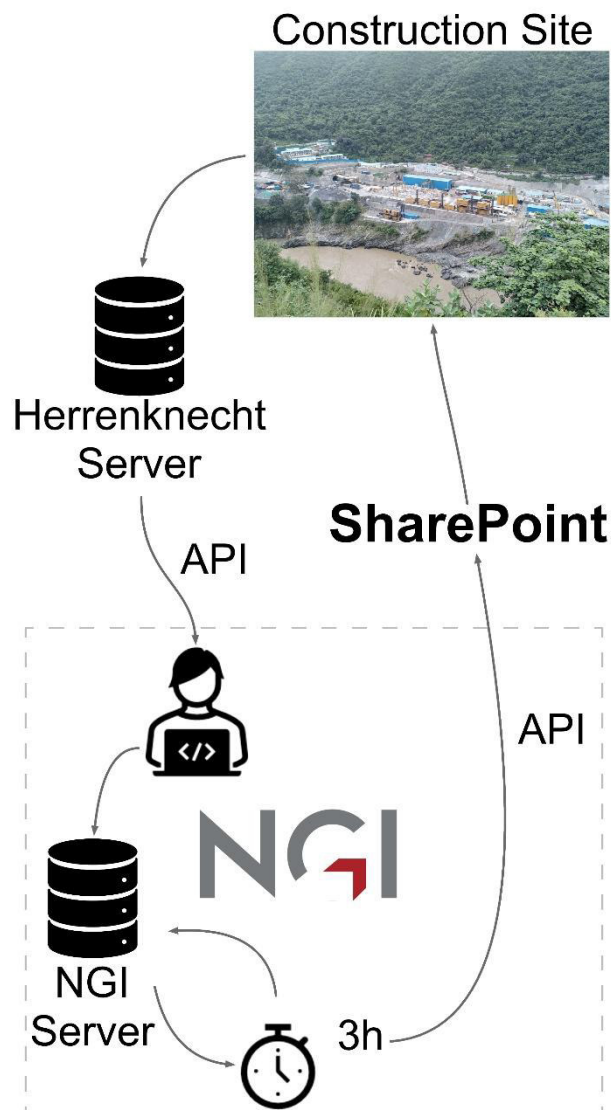
202 During excavation, actual ground conditions were systematically documented through daily
203 geological interpretation reports and site inspections. The TBMs Upline and Downline
204 encountered 21 and 14 water-bearing zones, respectively, with inflows typically ranging from 100–
205 200 L/min, which diminished over time. Although both tunnels exhibited comparable rock mass
206 characteristics, the Upline experienced higher water inflow due to its 300–700 m lead over the
207 Downline, facilitating preferential groundwater drainage. Despite comprehensive pre-
208 construction investigations, discrepancies arose between predicted and observed conditions,
209 notably in groundwater inflow and the occurrence of shear/fault zones.

210 18 and 11 fault zones were anticipated in the Upline and Downline, respectively, of which 11 and
211 8 were encountered. Most shear zones extended less than 10 m, except one major zone (~30 m).
212 Shear zones were identified using TBM operational parameters such as torque, total thrust,
213 contact force, penetration rate, and muck analysis. Notably, water-bearing zones at several
214 chainages corresponded closely with pre-construction predictions.

215 3. TBM Advance Monitoring Methodology

216 3.1. Data Analysis Framework

217 For continuous monitoring and analysis of TBM operational data during construction, a Python-
218 based data analysis framework was developed and iteratively enhanced throughout the project
219 (Figure 6, and detail in Figure 7). The implemented system operates in multiple sequential stages:
220 i) TBM operational data generated onsite is transmitted to Herrenknecht servers; ii) the data
221 analysis framework - hosted at NGI - accesses these servers automatically through an
222 application programming interface (API) to fetch the latest available data at intervals of ca. three
223 hours, processes incoming data and performs analyses; iii) the results are uploaded to a
224 SharePoint repository via a second API to make them accessible and viewable directly on-site.

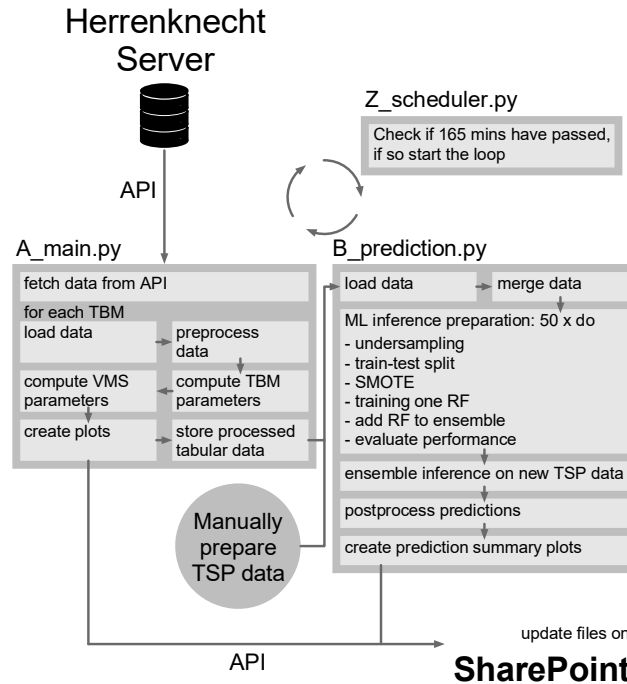


225

226 *Figure 6: Schematic showing the flow of the information in the developed TBM data analysis framework. The dashed*
227 *line indicates the detail view shown in Figure 7.*

228 The data analysis framework integrates multiple individual components of which conventional
229 TBM operational data monitoring, VMS-based squeezing risk prediction and ML- and geophysics-

230 based excavation condition predictions are the main ones that will be described in sections 3.2
 231 to 3.4 and assumptions and limitations are collected in section 3.5. A key strength of the overall
 232 framework is that it combines these components into one system to retrieve a holistic impression
 233 of the state of the TBM excavation rather than considering each one in isolation. A detailed view
 234 of the computational framework is shown in Figure 7 and pseudocode to reproduce the
 235 functionality is provided in the Code and Data availability section. The indicated functions and
 236 files in the pseudocode correspond to the elements in Figure 7.



237

238

Figure 7: Detailed view of the computational data analysis framework.

239 3.2. TBM Operational Data Monitoring

240 To retrieve a continuous and holistic picture of the excavation conditions on-site, advanced TBM
 241 data monitoring was done with the above-described framework. While direct TBM parameters
 242 such as the total thrust or the cutterhead torque provide valuable operational insights, several
 243 additional parameters were computed to retrieve a more nuanced picture of the system
 244 behavior. Click or tap here to enter text..

245 The performed TBM operational data preprocessing mostly follows the steps described in section
 246 3.1 to 3.3 of Erharter et al. (2025b) to which the reader is referred for in-depth information about
 247 the topic. Starting with 15 477 463 and 15 734 416 raw and unfiltered datapoints for the TBMs S-
 248 01309A and S-01310A, respectively, the datasets were reduced to the following numbers of
 249 datapoints in the preprocessing: 2 321 997 and 2 213 866 datapoints each, after basic data
 250 cleaning (i.e. standstill removal) which both are reductions of about 85% with respect to the raw
 251 data; 5986 and 5910 datapoints each, after spatial discretization (i.e. stroke-wise aggregation of
 252 the data), which are reductions of more than 99% with respect to the datasets after basic data
 253 cleaning. Note that especially the spatial discretization was not done for every step in the
 254 analysis, as some required detailed data and not just aggregations for each stroke. The following
 255 parameters were computed:

256 ▪ **Thrust Force Loss** (F_r): This parameter quantifies the difference between the total thrust
257 force applied by the TBM (F_T) and the effective advance force acting on the cutterhead
258 (F_a) and thus is indicative for the TBM's shield friction (Erharter et al., 2023). F_r is only
259 directly computable for TBMs that separately record both total thrust and advance force.

$$F_r = F_T - F_a \quad \text{eq. 1}$$

260 ▪ **Specific Penetration** (p_s): The specific penetration (Gong and Zhao, 2009) describes the
261 penetration per unit force and is calculated by dividing the penetration per cutterhead
262 rotation (in mm) (p) with F_a (eq. 2).

$$p_s = \frac{p}{F_a} \quad \text{eq. 2}$$

263 ▪ **Specific Excavation Energy** (e_r): Following Teale (1965), this parameter represents the
264 required energy input to excavate one unit volume of rock mass. It can be decomposed
265 into components related to thrust and rotation and especially the latter has shown good
266 correlation with the encountered rock mass conditions. As described by Bergmeister and
267 Reinhold (2017), low specific energy typically correlates with weak rock masses, while
268 high values indicate stronger materials. The rotational specific energy is calculated using
269 eq. 3, where A is the tunnel face area, N the number of cutterhead rotations and T the
270 cutterhead torque:

$$e_r = \left(\frac{2\pi}{A}\right) \left(\frac{NT}{p}\right) \quad \text{eq. 3}$$

271 ▪ **Torque Ratio**: Originally introduced by Radončić et al. (2014) (see also Erharter et al.
272 (2025b)), the torque ratio compares the measured cutterhead torque (T) to the theoretical
273 torque (M_{th}). It serves as an indicator of ground conditions and is the base for the data
274 driven advance classification now included in the Austrian TBM excavation standard
275 ÖNORM B2203-2 (Austrian Standards, 2023). It is calculated in the simple form according
276 to eq. 4 where F_t is the tangential force acting on the cutters, n_{disk} is the number of
277 cutters, D_{CH} is the cutterhead radius and M_0 is the idle torque required for cutterhead
278 rotation.

$$M_{th} \sim 0.3 * F_t * n_{disk} * D_{CH} + M_0 \quad \text{eq. 4}$$

279

280 3.3. Squeezing Risk Monitoring

281 In addition to the parameters described above, tunnel wall deformations were monitored
282 following the descriptions given in section 2.2, producing continuous tunnel wall deformation
283 profiles with measurements every 1.7 meters, which is unprecedented in this consistency in
284 shielded hard rock TBM tunnel construction. As the geology of the project features comparatively
285 soft rocks, overburdens of up to 860 meters and active tectonic stresses (sections 2.1 and 2.3),
286 the risk of squeezing rock mass was deemed to be considerable and a method to estimate the
287 current and continuously evolving squeezing risk was required.

288 Given a certain tunnel wall deformation rate (r_{def} [mm/h]) measured at the position of VMS 3 and
289 a certain size of the shield gap (s [mm]) at that position, the time (t_{close} [h]) in which this gap would
290 close can be computed by the following equation.

$$t_{close} = \frac{s}{r_{def}} \quad \text{eq. 5}$$

291 As standing still therefore unavoidably leads to getting stuck, the only option is to keep advancing.
292 It must be considered that t_{close} is measured at position of VMS 3 (i.e. not the end of the TBM),
293 and there is still some length of the shield behind this position that potentially also can get stuck,
294 termed l_s [m] ($l_s = 3.8$ m in case of the Rishikesh-Karnaprayag project, see Figure 5). Note that
295 determining s and l_s requires consideration of the conicity of the shield. The required minimum
296 gross advance speed (i.e. excavation speed including standstills, a_{gross_min} [m/h]) for the TBM to
297 avoid getting stuck can therefore be computed as l_s/t_{close} , which can also be expressed as
298 follows:

$$a_{gross_min} = \frac{l_s * r_{def}}{s} \quad \text{eq. 6}$$

299 It is thus possible to compute the minimum required gross advance speed and / or required
300 overcut to be able to "escape" a deforming tunnel wall and not get squeezed in given a fixed shield
301 length. Applying an overcut to increase s is, however, only possible in future strokes ahead of the
302 one where the measurement has been taken. Assumptions and limitations of the approach are
303 outlined in section 3.5. Although the relationship is derived from first-order kinematic arguments
304 rather than detailed plasticity models, it proved consistent with on-site observations: gross
305 advance speed always remained above minimum values required to avoid problems with a with
306 tunnel wall deformation rates and no squeezing incidents occurred (see section 4 and Figure 10).

307 3.4. Excavation Condition Prediction

308 As outlined in Figure 1, the other main task aside from squeezing risk monitoring was to predict
309 the excavation conditions ahead of the TBM to retrieve an early indication of upcoming adverse
310 ground conditions as decision support and early warning for the TBM operators. A supervised ML
311 solution was used to predict the excavation condition ahead of the TBM.

312 3.4.1. Rational of using Machine Learning

313 In accordance with Bozorgzadeh and Feng (2024) is it important to justify the use of ML which
314 should go beyond "*some data are available, and we know a class of algorithms for analyzing such*
315 *data*". The following reasons are given, and thus the ML application in the project complies with
316 the *Problem → Data → Algorithm* paradigm (Bozorgzadeh and Feng, 2024):

- 317 i) The notion of an *excavation condition* of a TBM by itself is conceptually challenging as it
318 is neither mechanistically nor physically well defined. While individual phenomena of the
319 TBM's excavation work can be understood with a physical understanding (e.g. a waning
320 cutterhead advance pressure when the TBM enters disturbed – softer – rock mass due to
321 reduced excavation resistance), the totality of the excavation condition is characterized
322 by different emergent phenomena resulting from the interaction of the TBM with the rock
323 mass (Erharter, 2026). Despite this complexity, onsite engineers are still able to determine
324 when the excavation is going well and when it does not, based on experience and
325 "engineering judgement". ML algorithms are thus seen as well suited for this prediction
326 task as their strong generalization capability permits synthetization of experience and
327 "engineering judgement".
- 328 ii) TBM excavations constitute one of the data-richest environments in all of geotechnical
329 engineering due to the high amount of data that is recorded by the TBMs. While this by
330 itself already lends itself to ML (Erharter et al., 2019; Erharter and Marcher, 2020), the

331 Rishikesh-Karnaprayag project was particularly well suited, as it had a wealth of data in
332 addition to the TBM operational data, first and foremost, regularly executed exploratory
333 drillings ahead of the TBM with measurement while drilling data (MWD) recording and
334 tunnel seismic predictions (TSP) that were executed from the TBM.

335 iii) The last years have seen a massive increase in the further development and application
336 of ML in general (Erharter, 2024) and there is consequently a plethora of algorithms to
337 choose from. For this particular task of sequential tabular data, an ensemble of Random
338 Forest algorithms was chosen as tree-based algorithms still are on-par with more
339 complex ML methods when it comes to this kind of data (Grinsztajn et al., 2022). More
340 detailed descriptions can be found below.

341 3.4.2. Conceptual Approach

342 To assign a quantitative label for the notion of “excavation condition”, a TBM-operational data
343 driven approach was used to classify the excavation in an objective and transparent manner. The
344 choice was made to use the binary TBM advance classification according to Radončić et al.
345 (2014) that discriminates either “regular” or “exceptional” excavation. This system is now also
346 implemented in the new Austrian Contractual Standard for underground excavation with TBMs:
347 the ÖNORM B2203-2 (Austrian Standards, 2023). Technicalities of this TBM advance
348 classification system are explained in detail in Erharter et al. (2025b). Aside from its data-driven
349 objectivity, another rational for this choice was the methodological problems from which many
350 other common, index based rock mass classification systems suffer (Erharter et al., 2024; Liu et
351 al., 2025).

352 Demands for the input data from which the excavation condition could be predicted were that it
353 i) comes from exploration data ahead of the TBM, ii) it contains the desired prediction information
354 in principle and iii) it must have a sufficiently high resolution to show adverse zones of interest. In
355 today’s tunnel excavation there are three main investigation measures that fulfill these
356 requirements: exploratory core drilling ahead of the face (not available here), exploratory
357 destructive (percussion) drilling ahead of the face with MWD data collection, and geophysical
358 exploration ahead of the face.

359 AsClick or tap here to enter text. MWD data was not usable for prediction (see section 3.5),
360 geophysical investigations ahead of the TBM were the used data source. In the Rishikesh-
361 Karnaprayag project, the TSP system from Amberg Technologies was used (Dickmann and
362 Groschup, 2010). The seismic source was an impact hammer installed on the TBM and
363 geophones were installed in boreholes behind the tunnel face to collect the reflected seismic
364 signals from structures ahead of the tunnel. The raw data from the geophones is converted to
365 usable information via geophysical data processing and seismic inversion. The TSP system then
366 yields geophysical parameters like P- or S-wave velocities or Poisson’s ratios ahead of the tunnel
367 face as an output. While these parameters are useful for people with a geophysical background,
368 they are not directly relatable to excavation conditions.

369 Bringing the two systems together, the overall ML concept at the Rishikesh-Karnaprayag project
370 was to use the predicted parameters from the TSP investigation as input to a ML model, and the
371 TBM data-based advance classification as output. This setup combines historical data of already
372 excavated parts of the tunnel and facilitates prediction of strokes that are potentially

373 “exceptional” ahead of the current tunnel face. Through this, the TBM operator can foresee if
374 upcoming strokes of the TBM will be regular or exceptional and hence be able to adapt the TBM
375 excavation accordingly.

376 3.4.3. Machine Learning Methodology

377 The supervised ML approach employed the Random Forest (Breiman, 2001) algorithm,
378 implemented as an ensemble of 50 independent classifiers effectively creating a “forest of
379 forests” or “rank 2” ensemble. Each Random Forest consisted of 100 decision trees, and the
380 ensemble diversity was achieved through using different random seeds for data sampling and the
381 randomization in the algorithm. As every single random forest yields a deterministic prediction,
382 based on its own interpretation of the training data, the goal of this ensemble of random forests
383 was to retrieve a probabilistic prediction of the expected excavation conditions based on how
384 well the ensemble members agree with each other.

385 The TSP derived geophysical parameters (P-wave velocity, S-wave velocity, Poisson ratio, static
386 Young’s modulus, dynamic Young’s modulus, shear modulus and bulk modulus) served as input
387 features while the binary advance classification labels (regular vs. exceptional) based on
388 thresholding torque ratios served as labels. Torque ratio values within the interval {0.65, 1.35}
389 were labeled regular, whilst values outside were considered exceptional. These threshold values
390 were set based on discussions with on-site personal so that they reflected experienced
391 exceptional excavation conditions like overbreaks and other challenges. As the threshold value
392 definition is decisive for the advance classification, it is imperative that this is done in close
393 collaboration with onsite personnel to ensure that it corresponds to the real state of the
394 excavation.

395 A critical challenge, which is also characteristic of these types of prediction problems, was the
396 inherent class imbalance in the dataset. Regular advances substantially outnumbered
397 exceptional advances. To address this whilst maintaining sensitivity to exceptional conditions, a
398 hybrid resampling strategy was implemented. First, the majority class (regular advances) was
399 under-sampled by removing 20% of the difference in class counts. Subsequently, the minority
400 class was over-sampled using the Synthetic Minority Over-Sampling Technique (SMOTE) (Chawla
401 et al., 2002) which generates synthetic samples by interpolating the features of data within the
402 minority class. This boosts the number of datapoints in the minority class to be the same as the
403 majority class.

404 The data was then split into a 3:1 stratified train-test split to preserve the class distributions. The
405 test dataset was used for evaluating the predictive capability of the model based on “confusion
406 matrices” normalized by the true class counts. In addition, feature importances were quantified
407 using SHAP (Shapely Additive explanations) values (Lundberg and Lee, 2017), offering insights
408 into which features were steering the predictions. In parallel, a separate ensemble model is
409 trained using the full dataset for forward predictions. To prevent unrealistic changes from the
410 TBM’s current state to the upcoming strokes, the four upcoming strokes were naively predicted
411 from the last observed stroke, with gradually decreasing weights of 0.9:0.1, 0.7:0.3, 0.4:0.6 and
412 0.1:0.9, respectively.

413 The ML based predictions of advance conditions ahead of the TBM were embedded in the overall
414 data processing framework as described in section 3.1. Due to the integration in the continuously
415 running data processing framework, ensemble models were frequently retrained with a growing
416 dataset thus continuously improving prediction quality.

417 3.5. Assumptions and Limitations

418 The computational methods deployed at the Rishikesh-Karnaprayag project are subject to
419 several conditions outlined below that need to be considered when the methods are to be reused
420 in future projects. The following assumptions were made.

- 421 ▪ The TBM data processing (section 3.2) assumes that the measured and computed
422 parameters are representative for the properties and phenomena of interest (Erharter,
423 2026).
- 424 ▪ Interaction effects between the two tunnels (e.g. stress redistributions, drainage, etc.)
425 were not considered as there were no indications that these phenomena have had a
426 significant effect onto the analyses.
- 427 ▪ The relationship for VMS-based squeezing risk monitoring presented in section 3.3
428 assumes that: i) deformations are isotropic, thus displacements are equally distributed
429 around the tunnel periphery, ii) the tunnel wall deformation rate is linear over time. While
430 deformations in conventional tunneling are known to be decreasing (Schubert et al.,
431 2014), was this considered to be justified as it increases conservatism and to avoid
432 introducing additional assumptions about the rock mass behavior; iii) if squeezing
433 occurs, the TBM gets squeezed in from the tail as the tunnel has had the longest time to
434 deform there.

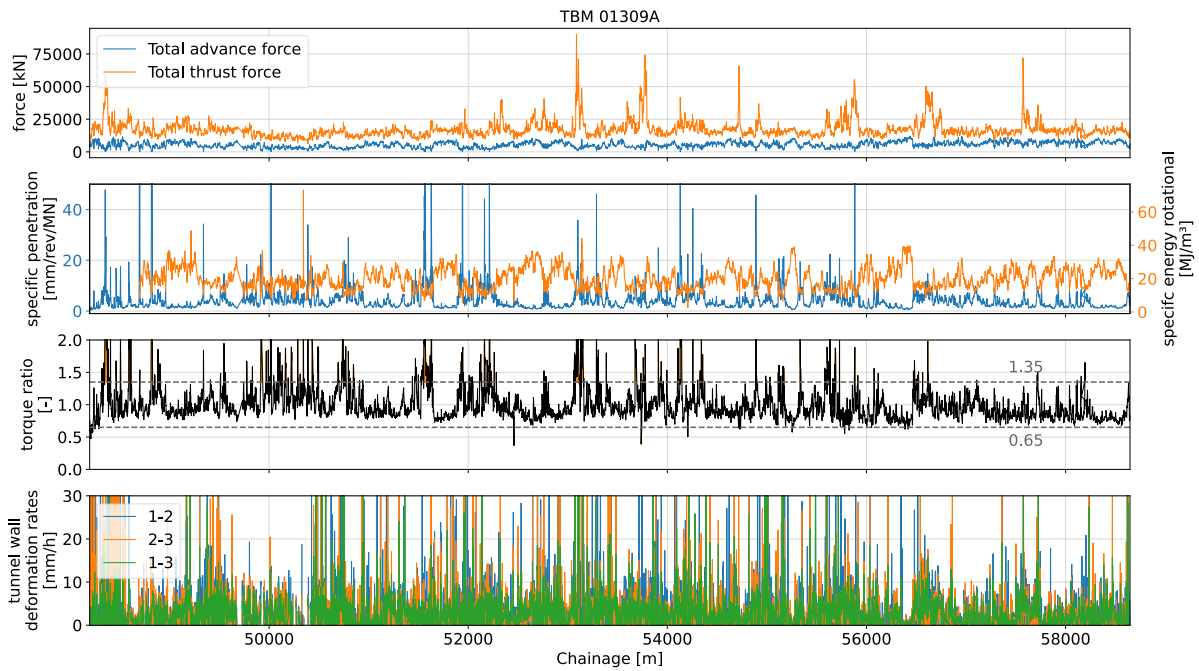
435 In addition to assumptions, the computational methods are subject to several limitations:

- 436 ▪ A comprehensive computational framework as presented uses dozens of interdependent
437 hyperparameters such as: i) torque ratio bounds of 0.65 and 1.35 (section 4); ii) filtering
438 of VMS data based on the 5 cm criterion (end of section 2.2); iii) preprocessing decisions
439 like using the arithmetic mean to aggregate datapoints for whole strokes (Erharter et al.,
440 2025b); iv) ML hyperparameters, like the under-sampling ratio, number of predictive
441 models in the predictive ensemble (section 3.4). As the framework was set up during an
442 ongoing project and had to deliver results from the start, systematic parameter-sensitivity
443 study was infeasible, as opposed to many academic exercises that are only done in
444 retrospective and datasets are final. The set parameters were therefore overwhelmingly
445 set by trial and error, starting from default values and or experience. Where parameters
446 filter out datapoints, the set values reflect tradeoffs between removing noise and outliers
447 and removing too many datapoints. It is nevertheless recommended to do parameter
448 sensitivity studies when a project allows for it.
- 449 ▪ No specific measures have been taken to quantify or address autocorrelation of data. As
450 the project was ongoing and data came in constantly, addressing these aspects would
451 have required implementation in the pipeline as automated preprocessing, which is non-
452 trivial. Not addressing this has the implication that the effective dataset size of the is
453 lower than the total one. It is implicit in the proposed solution that similar TSP inputs
454 should reflect similar ML outputs. Therefore, redundancies in acquired TSP data should

- 455 be seen as a benefit, indicating that similar conditions have been encountered prior in the
456 excavation leading to higher confidence in the prediction.
- 457 ■ The fact that the VMS is installed on one side of the shield only (Figure 4b) requires the
458 above-given assumption of isotropic rock mass deformation. This is a noteworthy
459 limitation in anisotropic rocks and ideally one would install two symmetrical rows of VMS
460 on both sides of the TBM's shield.
 - 461 ■ MWD data was the originally preferred input for ML predictions (section 3.4.2) due to prior
462 positive experiences (Hansen et al., 2024a). Several attempts were made to use the
463 collected MWD data from the construction site for predictions, but the results were not
464 satisfactory as the data quality was insufficient due to inconsistent and unreconcilable
465 drilling. For MWD data to be used successfully for predictions (e.g. as practiced at
466 Scandinavian tunnel construction sites) it must be collected in a highly consistent
467 manner (e.g. keeping all but one parameter constant, to ensure that a proper signal of the
468 rock mass is retrieved).
 - 469 ■ With respect to today's ML best-practice recommendations like the one proposed by
470 Erharter et al. (2025a), it can be said that the majority of requirements in the categories
471 ML "*prototyping*" and "*publishing standards*" are fulfilled, except for the "*Dataset and*
472 *Experiment Control*" which demands full versioning of all past models and data-subsets
473 to ensure full reproducibility of results at any time. This was not done in the project due to
474 practical reasons and time constraints. In principle, however, having version control that
475 goes beyond the used code is highly encouraged for future projects where eventually
476 decision critical predictions are made.

477 4. On-site observations and experiences

478 The continuous monitoring of TBM operational data, described in sections 3.1 and 3.2 permitted
479 retrieving a holistic picture of the state of the construction site remotely. The first row in Figure 8
480 shows the measured thrust (i.e. the force exerted by the TBMs' thrust cylinders) and the advance
481 force (i.e. the force the cutterhead exerts on the tunnel face). These are interpreted to be
482 indicative for the frictional loss that occurs as the TBM moves through the tunnel (Erharter et al.,
483 2023). An increasing thrust force, without an increase in advance force thus means that there is
484 increased shield friction, potentially indicative of squeezing conditions or that rock blocks are
485 jammed in the shield gap due to an unstable tunnel wall. The second row shows the computed
486 specific penetration and specific excavation energy. These parameters are negatively correlated
487 with one another, and it can, for example, be seen how the specific excavation energy is high,
488 when the thrust force is comparatively low and stable. This is interpreted as a sign of strong rock
489 mass conditions and a stable tunnel wall, whereas spiking specific penetration is seen as a sign
490 for rock mass of heterogeneous quality as the TBM enters and leaves zones of stronger and
491 weaker rock mass. The third row shows the torque ratio after Radončić et al. (2014) and threshold
492 values to differentiate regular from exceptional strokes (here 0.65 and 1.35). The thresholds were
493 continuously updated as the excavation progressed which is in line with the ÖNORM B 2203-2
494 and recent literature (Erharter et al., 2025b). Torque ratio spikes above 1.35 align reasonably well
495 with the above-described indicators for weaker, heterogeneous and less stable rock masses,
496 thus further strengthening the holistic picture retrieved from the data.

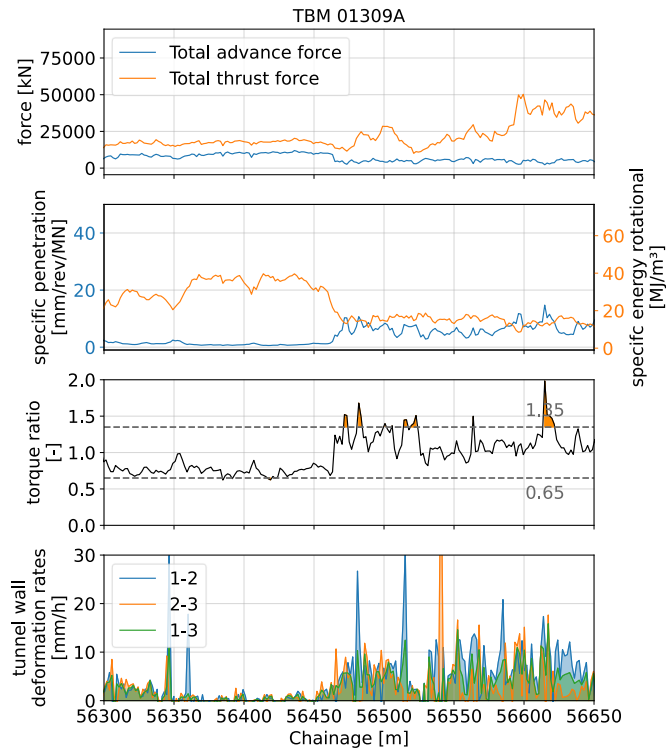


497

498 *Figure 8: Analyzed TBM operational data for one of the TBMs at the Rishikesh-Karnaprayag project.*

499 The fourth row in Figure 8 shows VMS-based tunnel wall deformation rates as described in section
500 3.3. Note that there are three deformation rates shown: VMS1 - VMS2, VMS2 - VMS3 and VMS1 -
501 VMS3. For further analyses, the deformation rate between VMS1 to VMS3 was used as this is seen
502 as the one that best represents the deformation rate over all three VMSs. In comparison to the
503 other TBM operational data, this signal is noisier, which is related to the sensitivity to the TBM's
504 position (Figure 5b). Nevertheless, the underlying pattern does correlate with the other above-
505 described indicators that describe the excavation condition, and it frequently was observed that
506 elevated deformation rates go along with weaker rock mass conditions.

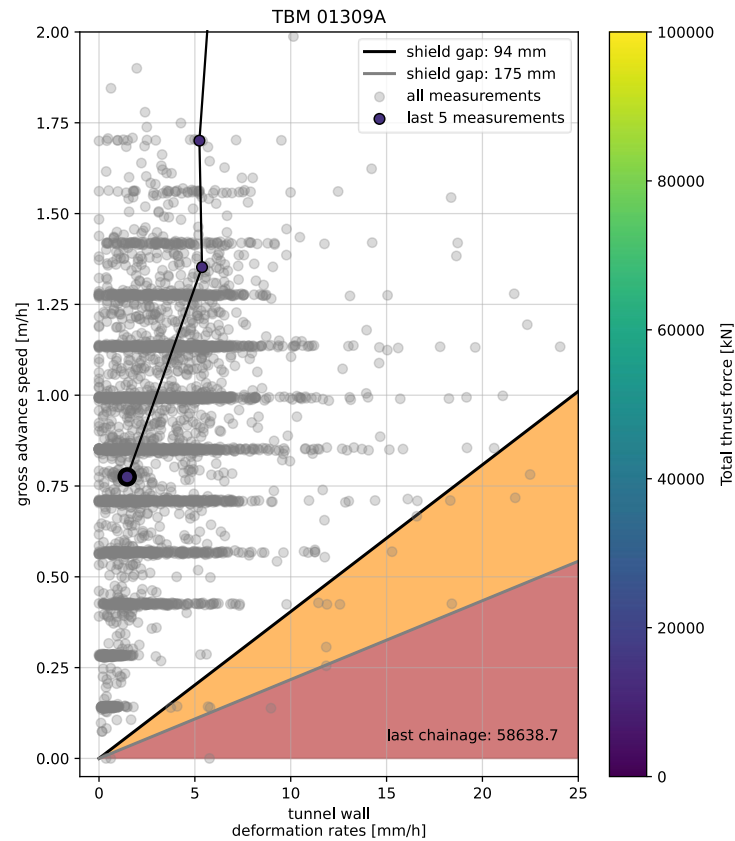
507 A detailed view onto one zone where a transition from favorable to less favorable rock mass
508 conditions was encountered by TBM 01309A at about chainage 56450 is shown in Figure 9. As the
509 TBM enters less favorable conditions, it can be well seen how the advance force decreases while
510 the thrust force increases, specific rotational energy decreases, specific energy increases, the
511 torque ratio increases on average and becomes spikey and also the VMS shows increased tunnel
512 wall deformation rates.



513

514 *Figure 9: Detail view of the TBM operational data where favorable rock mass conditions are encountered up to ca.*
 515 *chainage 56450 und less favorable ones afterwards.*

516 As described in section 3.3, a special squeezing risk early warning system was developed that
 517 utilizes the tunnel wall deformation rates beyond what is shown in Figure 8 and Figure 9. Figure
 518 10 shows one such squeezing risk assessment where the tunnel wall deformation rate as
 519 measured by the VMS system is on the x-axis and the gross advance speed on the y-axis. The
 520 diagonal lines that delimit the orange and red sections are computed with eq. 6 and indicate
 521 minimum gross advance speeds that are required to avoid getting stuck, given a certain tunnel
 522 wall deformation rate and the fixed length of the shield. The difference between orange and red is
 523 the size of the shield gap, where the former shows the standard shield gap and the latter a
 524 widened shield gap due to an applied overcut. The grey dots indicate all past states of the TBM
 525 excavation within this diagram and the last 5 strokes are indicated by bold dots, to show how the
 526 TBM is doing right now. If the TBM's current status (bold points) would move into the orange or red
 527 shaded area, this can be interpreted as a higher risk for the TBM to get stuck due to squeezing
 528 rock mass. It can be seen that the vast majority of TBM states are in the safe area and the ones
 529 within the orange / red zone can be attributed to outliers and measuring errors.



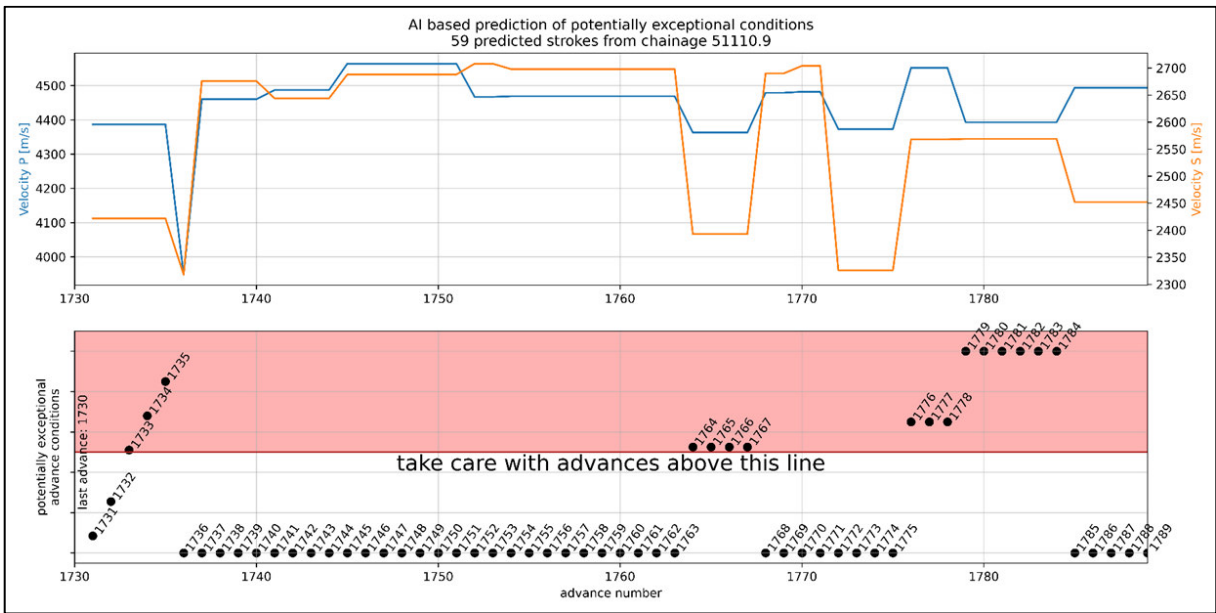
530

531 *Figure 10: Novel methodology to predict the risk of squeezing in the shield area of a hard rock TBM, that relates the*
 532 *parameters tunnel wall deformation rate, TBM gross advance speed, length of the TBM shield and size of the shield gap.*
 533 *Orange and red areas indicate zones of elevated squeezing risk*

534 The ML and TSP-based predictions of the expected excavation conditions ahead of the TBM
 535 yielded a classification of 0 = regular excavation and 1 = exceptional excavation. An exemplary,
 536 final prediction ahead of the cutterhead is shown in Figure 11. The upper row of Figure 11 shows
 537 the exemplary TSP parameters V_p and V_s . The lower row shows “potentially exceptional advance
 538 conditions” ahead of the last available position of the TBM. The prediction goes as far as the TSP
 539 reaches ahead of the current position and is consequently subject to change as the TBM
 540 advances. The strokes ahead are annotated with their respective stroke numbers. The scale of
 541 the y-axis corresponds to 0 (regular stroke) and 1 (exceptional stroke). A predicted stroke that
 542 plots above the red line (i.e., 0.5) is potentially exceptional and additional care when excavating
 543 this stroke should be applied. The height of the point above the red line gives a certain indication
 544 about the model uncertainty with respect to whether or not a stroke can be classified as “regular”
 545 or “exceptional”. The model uncertainty is computed based on the ensemble of random forests
 546 (i.e. the forest of forests) and, for example, a value of 0.7 for a stroke means that 70% of the
 547 random forests predicted that the stroke will be exceptional, but 30% predicted that it will be
 548 regular. The 0-1 y-axis labels in the second row were deliberately omitted to avoid
 549 overinterpretation on the TBM operators’ side who were the end users of this analysis.

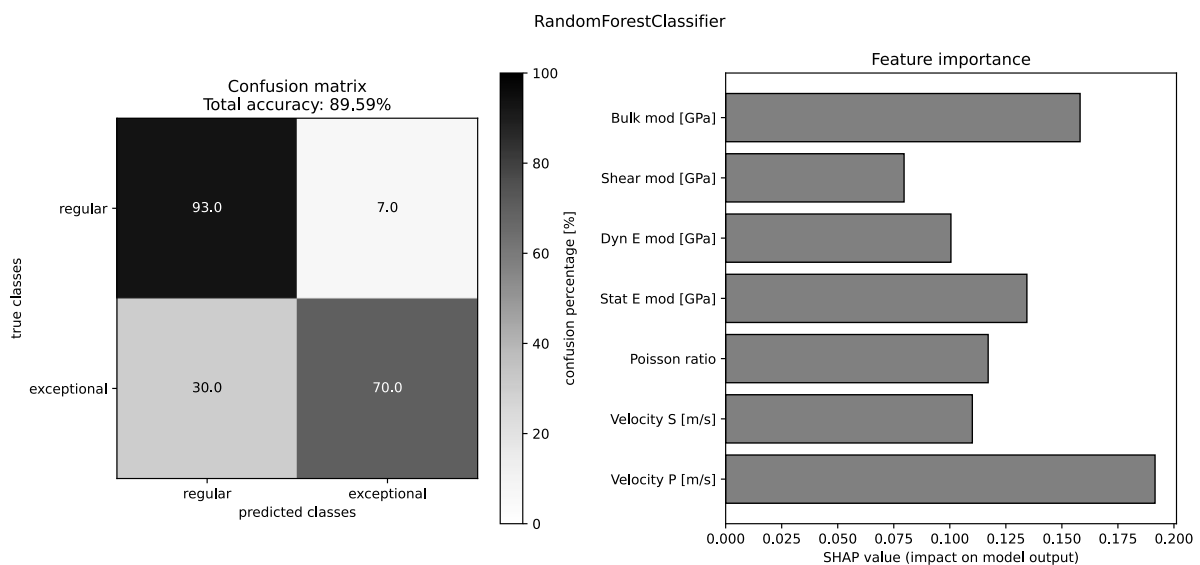
550 The performance of the ML prediction, along with a feature importance plot is shown in Figure 12.
 551 The left part of the figure represents performance evaluation as i) the “accuracy metric” holding
 552 a value of 89.59 % and ii) the row normalized confusion matrix showing how the proportion of true
 553 classes get predicted by the model. On the right side of the plot the SHAP feature importance

554 gives an indication of which features were considered important for the prediction outcomes
 555 (Lundberg and Lee, 2017). The clear difference between the prediction performance for the
 556 exceptional advance compared to the regular advance reflects the class imbalance present for
 557 the respective classes. However, the undersampling and oversampling significantly boosted the
 558 prediction performance for the minority class. The SHAP values indicate that the two driving
 559 features for predictions were the P-wave velocity and Bulk modulus computed from the TSP data.
 560 This indicates that there is a site-specific correlation to these parameters that gives a good
 561 indication of exceptional advance conditions.



562
 563 *Figure 11: Exemplary output of the ML prediction ahead of the TBM.*

564



565
 566 *Figure 12: Performance of a Random Forest Classifier for binary rock classification (regular vs. exceptional). (Left)*
 567 *Confusion matrix showing per-class prediction rates; overall accuracy is 89.59%. (Right) SHAP-based feature*
 568 *importance indicating that seismic P wave velocities and elastic Bulk modulus are the dominant predictors.*

569 5. Discussion

570 While TBM operational data processing is becoming a standard tool and is done on most
571 construction sites in one way or another, the Rishikesh-Karnaprayag project stands out as its
572 advanced TBMs were equipped with a plethora of sensors that enabled unprecedented
573 possibilities for data analysis. Systems like the VMS proved highly valuable to get an idea about
574 the conditions of the shield gap around the TBM, which is often one of the biggest points of
575 uncertainty in excavations with single- or double shield TBMs. Analyses like those of the VMS
576 data, however, also show that advanced TBM sensors and hardware are required to facilitate
577 comprehensive TBM data monitoring that allows to derive the system behavior. Both the software
578 (i.e. the data processing framework) and the hardware (i.e. the TBM) must be sufficiently
579 advanced to allow for advanced analyses.

580 The TBM operational data processing framework that was developed for the Rishikesh-
581 Karnaprayag project demonstrated how it can be possible to retrieve a holistic impression of the
582 ongoing excavation conditions onsite from a remote office. The chosen update frequency of 3
583 hours could have been reduced (to, e.g. < 1 hour) but this was not necessary based on the overall
584 excavation progress. In principle, systems like the presented ones could provide analyses and
585 predictions in near-to-real-time, but an hourly frequency is sufficient for today's excavation
586 performance.

587 The developed early warning squeezing-risk method is novel and can be used to strengthen risk
588 management for future shielded TBM excavations that employ systems like the given VMS. Even
589 though there never were any severe incidents relatable to squeezing, the VMS system yielded
590 valuable tunnel wall deformation data that could have been indicative for the current squeezing
591 risk (on a stroke by stroke basis) in a data-driven way. The fact that real squeezing incidents could
592 have been avoided is in principle positive for the excavation but also limits to which extent the
593 developed squeezing risk prediction chart's validity can be quantified as there were no "true
594 positives". Instead, the model can only be assessed based on its internal conceptual consistency
595 and on how the observed TBM states populate the diagram throughout excavation. With respect
596 to that good agreement was given.

597 In section 3.5, it was described that an initial attempt to use MWD data as the input for the ML
598 predictions was futile due to insufficient data quality. Even if the deployed sensors are of high
599 quality and technologically advanced, the way in which they are operated also has a substantial
600 influence on the final data. If either the primary data collection is flawed due to insufficient
601 sensors, or operational processes disturb the data collection, any further analyses may be futile.
602 Even the most advanced processing techniques are just tools to elicit information that must be
603 inherently hidden in the data. If the original dataset lacks the necessary quality or completeness,
604 no algorithm, however advanced, can compensate for that deficiency and ultimately, the
605 incentive to provide high quality data often hinges on the contractual boundary conditions.

606 Nevertheless, in the case of the Rishikesh-Karnaprayag project, the fully data driven ML-
607 prediction system was a success. The use of TSP data as input, and a binary classification of
608 excavation conditions based on the torque ratio as output, has shown to be an efficient and
609 functioning way of predicting advance conditions. Both data sources proved to be well suited for

610 this purpose. It is still emphasized that the ML system was designed as a decision support and
611 early warning tool for the TBM operator and not as the single true predictor of what is ahead of the
612 TBM. The chosen ML approach was algorithmically simple (i.e. no deep ML), but produced sound
613 predictions given the available data. It might have been possible to achieve higher classification
614 performances using different algorithms and systematic hyperparameter optimization
615 frameworks like Optuna (Akiba et al., 2019). The progressively increasing amount of data as the
616 TBMs advanced, however, showed to yield the largest performance increases and thus the focus
617 was rather put on improving the data processing framework than fine-tuning the ML models. [Click](#)
618 [or tap here to enter text.](#)

619 Like all predictive systems, both the squeezing risk prediction and the ML-based predictions of
620 excavation conditions represent trade-offs between being producing false alarms versus missing
621 actual unfavorable conditions. Due to the severe implications of a standstill due to a TBM getting
622 jammed by squeezing (i.e. up to months of project delay), the squeezing risk prediction system
623 was purposely designed to be conservative through assumptions like linear tunnel deformation
624 (section 3.5). This unavoidably led to several occasions where there was concern that an adverse
625 situation might be at hand, however, only increased communication and closer monitoring of the
626 excavation progress was the consequence of that, but no unnecessary measures were
627 implemented. As the ML-based excavation condition prediction system only gave an indication
628 to the TBM operator when they need to take extra care in driving the machine (Figure 11), no
629 particular delays or other consequences resulted from warnings of that system. All in all, the
630 developed data analysis framework had the positive effect that it increased the communication
631 between client, contractor and consultants onsite and explicitly drew attention to potentially
632 adverse excavation conditions.

633 6. Conclusion, Recommendations and Outlook

634 Tunnel construction is an answer to society's need for rapid rail and road connection, pathways
635 for water and energy, and security concerns. Advanced data analysis can substantially aid this
636 endeavor, but it is no "plug and play" process and has requirements with respect to data quantity
637 and quality. Nevertheless, it permits us to get a comprehensive and holistic impression of the
638 ongoing processes at a construction site in general and can also answer very specific questions
639 related to geotechnical risks such as squeezing. By that, a tunnel construction site can be
640 operated more efficiently, safer and more economical as data processing systems like the one
641 presented here help to avoid severe incidents.

642 The herein described developments that were done as part of the Rishikesh-Karnaprayag project
643 had the two goals to i) develop a data-centric squeezing risk prediction system and ii) develop a
644 system to predict the excavation conditions ahead of the TBM (Figure 1). Both were met by
645 developing new means of analytical or ML-based data analysis. The squeezing risk prediction
646 was, however, mainly facilitated by the availability of VMS data. The prediction of the excavation
647 conditions ahead of the tunnel face mainly depends on the availability of some exploratory
648 investigations such as MWD data or a TSP-like system. Future implementations of approaches
649 like these are possible in comparable excavation conditions, however, hinge on the availability of
650 these sources of information.

651 The following recommendations can be given for future similar projects:

- 652 - All desired data collection endeavors should be included in the construction site contract
653 to ensure that all data is collected with sufficient quality and that no other incentives
654 interfere with data collection quality.
- 655 - All information on-site should be collected digitally so that rapid access and sharing of it
656 is possible.
- 657 - TBM operational data processing should be done in a code-based manner to ensure
658 efficiency and (internal) reproducibility of results.
- 659 - In contrast to conventional consulting jobs, data-driven consulting as presented has a
660 comparatively high work effort in the beginning of the project as a code framework needs
661 to be set up, but this decreases over time once systems are up and running. This needs
662 to be considered on both the client's and consultant's side at project start.
- 663 - While the state-of-the-practice in retrieving TBM operational data today is still through
664 web interfaces and dashboards, accessing data programmatically through an API is a
665 prerequisite for any large scale and especially automatic analyses.
- 666 - If ML is to be used, the focus should be on the data quantity and quality and not using the
667 most advanced algorithms available.
- 668 - If MWD data is to be used for explorative purposes, it must be acquired in a systematic
669 and controlled manner, so that patterns in the data are representative for the material that
670 is drilled through and not for the drilling operation itself.
- 671 - A VMS system can provide vital information for shielded TBM excavations in potentially
672 squeezing rock mass, and more widespread use of VMS and documentation of
673 measurement results is encouraged. This will enable future research related to rock mass
674 behavior and ultimately better management of squeezing risk.

675 It must be considered that the rock mechanical observations and interpretations of the
676 Rishikesh-Karnaprayag project are confined to single-shield hard rock TBM excavations in
677 potentially squeezing rock mass in geology comparable to mountain ranges like the lesser
678 Himalayas. Nevertheless, with all the developments presented in this paper, the Rishikesh-
679 Karnaprayag project stands out as a role model for data-driven hard rock TBM excavation
680 monitoring and tunnel innovation in a practical project.

681 The most important next step in this development is to test the framework on other TBM
682 construction sites that also use a TSP system. In a bigger picture, large development potential is
683 seen in establishing databases of TBM construction sites that include the TBM operational data,
684 labels like geological tunnel documentation, cutter wear protocols and other data such as
685 seismic predictions. This would enable a multitude of follow up studies in various different
686 directions, including but not limited to statistical analyses of TBM data, integration with
687 numerical modeling, retrospective uncertainty analyses with respect to the expected conditions
688 and others. This development should be done in close collaboration of academia and industry
689 and push the mechanized tunneling community forward as a whole.

690 Code and Data availability

691 The full code and data of the project cannot be shared due to confidentiality. The reader is
692 referred to Erharter et al. (2025b) where similar code for TBM data processing is provided in the

693 appendix. Pseudocode for the herein described framework can be found in the attached file
694 Rishikesh_pseudocode.md

695 Acknowledgments

696 The Norwegian Geotechnical Institute has provided open access funding for this article.

697 Author Contributions

698 **Georg Erharter:** Conceptualization, Data curation, Formal analysis, Investigation, Methodology,
699 Project administration, Software, Supervision, Visualization, Writing – original draft

700 **Sumit Jain:** Investigation, Resources, Validation, Writing – original draft

701 **Øyvind Dammyr:** Conceptualization, Data curation, Investigation, Methodology, Software,
702 Visualization, Writing – review & editing

703 **Sjur Beyer:** Conceptualization, Data curation, Formal Analysis, Investigation, Methodology,
704 Software, Visualization, Writing – original draft

705 **Rajinder Bhasin:** Funding acquisition, Project administration, Supervision, Writing – review &
706 editing

707

708 References

709 Akiba, T., Sano, S., Yanase, T., Ohta, T., Koyama, M., 2019. Optuna: A Next-generation
710 Hyperparameter Optimization Framework, in: Proceedings of the 25th ACM SIGKDD
711 International Conference on Knowledge Discovery & Data Mining. KDD '19: The 25th ACM
712 SIGKDD Conference on Knowledge Discovery and Data Mining, Anchorage AK USA. 04 08
713 2019 08 08 2019. ACM, New York, NY, USA, pp. 2623–2631.

714 Austrian Standards, 2023. Untertagebauarbeiten ÖNORM B 2203-2:2023 03 01: Teil 2:
715 Kontinuierlicher Vortrieb 91.010.20; 93.020, 60 pp.

716 Barla, G., 2001. Tunnelling under squeezing rock conditions, in: Eurosummer-School in Tunnel
717 Mechanics. Logos Verlag, pp. 169–268.

718 Bergmeister, K., Reinhold, C., 2017. Learning and optimization from the exploratory tunnel -
719 Brenner Base Tunnel. Geomechanics and Tunnelling 10 (5), 467–476.
720 <https://doi.org/10.1002/geot.201700039>.

721 Bianchi, G.W., 2023. Analysis of TBM parameters during tunnelling in adverse conditions – The
722 case study of the Frejus Safety Tunnel, Western Alps. Geomechanics and Tunnelling 16 (1),
723 47–52. <https://doi.org/10.1002/geot.202200070>.

724 Bieniawski, Z.T., 1973. Engineering Classification of Jointed Rock Masses. Civil Engineer in South
725 Afrika 15 (12), 335–343.

726 Bobet, A., Einstein, H.H., 2024. Tunnel design methods. CRC Press Taylor & Francis Group, Boca
727 Raton, London, New York, 611 pp.

- 728 Bozorgzadeh, N., Feng, Y., 2024. Evaluation structures for machine learning models in
729 geotechnical engineering. *Georisk: Assessment and Management of Risk for Engineered*
730 *Systems and Geohazards* 18 (1), 52–59. <https://doi.org/10.1080/17499518.2024.2313485>.
- 731 Breiman, L., 2001. Random Forests. *Machine Learning* 45 (1), 5–32.
732 <https://doi.org/10.1023/A:1010933404324>.
- 733 Chawla, N.V., Bowyer, K.W., Hall, L.O., Kegelmeyer, W.P., 2002. SMOTE: Synthetic Minority Over-
734 sampling Technique. *Jair* 16, 321–357. <https://doi.org/10.1613/jair.953>.
- 735 Dickmann, T., Groschup, R., 2010. Tunnel seismic exploration and its validation based in data
736 from TBM control and observed geology. In: Beer, G. (Ed.), *Technology innovation in*
737 *underground construction*. CRC Press/Taylor & Francis, Boca Raton, Fla.
- 738 Erharter, G.H., 2024. Digitally Empowered Geo-Engineering Toolbox: From AI-Driven Lab Data
739 Interpretation, BIM Ground Modelling to Parametric Design. In: Gutierrez, M. (Ed.),
740 *Information Technology In Geo-Engineering. Proceedings of the 5th International Conference*
741 *on Information Technology in Geo-Engineering ICITG 2024*. SPRINGER INTERNATIONAL PU,
742 [S.l.], pp. 199–208.
- 743 Erharter, G.H., 2026. Keynote lecture From Bits to Bytes: Deciphering System Behavior through
744 TBM Data. Monash University. *Joined Conferences on CTTU & TBM DiGs*, 23 January 2026,
745 Melbourne, Australia.
- 746 Erharter, G.H., Bar, N., Hansen, T.F., Jain, S., Marcher, T., 2024. International Distribution and
747 Development of Rock Mass Classification: A Review. *Rock Mech Rock Engng.*
748 <https://doi.org/10.1007/s00603-024-04215-8>.
- 749 Erharter, G.H., Goliash, R., Marcher, T., 2023. On the Effect of Shield Friction in Hard Rock TBM
750 Excavation. *Rock Mech Rock Engng.* <https://doi.org/10.1007/s00603-022-03211-0>.
- 751 Erharter, G.H., Hansen, T.F., Høivang, G.P., Beyer, S., Liu, Z., 2025a. NGI Machine Learning Best
752 Practices Checklist - Process Pipeline. Norwegian Geotechnical Institute.
753 [https://www.researchgate.net/publication/388322984_NGI_Machine_Learning_Best_Practi](https://www.researchgate.net/publication/388322984_NGI_Machine_Learning_Best_Practices_Checklist_-_Process_Pipeline)
754 [ces_Checklist_-_Process_Pipeline](https://www.researchgate.net/publication/388322984_NGI_Machine_Learning_Best_Practices_Checklist_-_Process_Pipeline) (accessed 10 March 2025).
- 755 Erharter, G.H., Marcher, T., 2020. MSAC: Towards data driven system behavior classification for
756 TBM tunneling. *Tunnelling and Underground Space Technology* 103, 103466.
757 <https://doi.org/10.1016/j.tust.2020.103466>.
- 758 Erharter, G.H., Marcher, T., Reinhold, C., 2019. Application of artificial neural networks for
759 Underground construction – Chances and challenges – Insights from the BBT exploratory
760 tunnel Ahrental Pfons. *Geomechanics and Tunnelling* 12 (5), 472–477.
761 <https://doi.org/10.1002/geot.201900027>.
- 762 Erharter, G.H., Unterlass, P., Radončić, N., Marcher, T., Rostami, J., 2025b. Challenges and
763 Opportunities of Data-Driven Advance Classification for Hard Rock TBM excavations. *Rock*
764 *Mech Rock Engng.* <https://doi.org/10.1007/s00603-025-04542-4>.
- 765 Gong, Q.M., Zhao, J., 2009. Development of a rock mass characteristics model for TBM
766 penetration rate prediction. *International Journal of Rock Mechanics and Mining Sciences* 46
767 (1), 8–18. <https://doi.org/10.1016/j.ijrmms.2008.03.003>.
- 768 Grinsztajn, L., Oyallon, E., Varoquaux, G., 2022. Why do tree-based models still outperform deep
769 learning on tabular data?, in: *6th Conference on Neural Information Processing Systems*
770 *(NeurIPS 2022). Track on Datasets and Benchmarks*, New Orleans.

- 771 Hansen, T.F., Erharter, G.H., Liu, Z., Torresen, J., 2024a. A comparative study on machine
772 learning approaches for rock mass classification using drilling data. *Applied Computing and*
773 *Geosciences* 24, 100199. <https://doi.org/10.1016/j.acags.2024.100199>.
- 774 Hansen, T.F., Erharter, G.H., Marcher, T., 2024b. Towards reinforcement learning - driven TBM
775 cutter changing policies. *Automation in Construction* 165, 105505.
776 <https://doi.org/10.1016/j.autcon.2024.105505>.
- 777 Hoek, E., Brown, E.T., 1997. Practical estimates of rock mass strength. *International Journal of*
778 *Rock Mechanics and Mining Sciences* 34 (8), 1165–1186. [https://doi.org/10.1016/S1365-
779 *1609\(97\)80069-X*.](https://doi.org/10.1016/S1365-1609(97)80069-X)
- 780 Liu, J., Feng, Y., Jiao, Y., 2025. The Phlogiston Theory of Rock Mass Classification: Philosophical
781 and Mathematical Critique of Ordinal Data Usage. *Rock Mechanics Bulletin*, 100205.
782 <https://doi.org/10.1016/j.rockmb.2025.100205>.
- 783 Lundberg, S.M., Lee, S.-I., 2017. A Unified Approach to Interpreting Model Predictions,
784 in: *Advances in neural information processing systems* 30. 31st Annual Conference on
785 *Neural Information Processing Systems (NIPS 2017)* : Long Beach, California, USA, 4-9
786 December 2017. Curran Associates Inc, Red Hook, NY.
- 787 Maidl, B., Schmid, L., Ritz, W., Herrenknecht, M., 2008. *Hardrock tunnel boring machines*. Ernst,
788 Berlin, 343 pp.
- 789 Maidl, B., Thewes, M., Maidl, U., Sturge, D., 2013. *Handbook of tunnel engineering*, 1st ed.
790 Ernst/Wiley, Berlin, 454 pp.
- 791 Radončić, N., Hein, M., Moritz, B., 2014. Determination of the system behaviour based on data
792 analysis of a hard rock shield TBM. *Geomechanics and Tunnelling* 7 (5), 565–576.
793 <https://doi.org/10.1002/geot.201400052>.
- 794 Ramoni, M., Anagnostou, G., 2010. Tunnel boring machines under squeezing conditions.
795 *Tunnelling and Underground Space Technology* 25 (2), 139–157.
796 <https://doi.org/10.1016/j.tust.2009.10.003>.
- 797 Ramoni, M., Anagnostou, G., 2011. The Interaction Between Shield, Ground and Tunnel Support
798 in TBM Tunnelling Through Squeezing Ground. *Rock Mech Rock Eng* 44 (1), 37–61.
799 <https://doi.org/10.1007/s00603-010-0103-8>.
- 800 Schubert, W., Grossauer, K., Matt, R., Bernd, M., Proprenter, M., Rabensteiner, K., Radoncic, N.,
801 Vavrovsky, G.M., Weissnar, M., 2014. *Geotechnical Monitoring in Conventional Tunnelling:*
802 *Handbook*. Austrian Society for Geomechanics, Salzburg, 96 pp.
- 803 Teale, R., 1965. The concept of specific energy in rock drilling. *International Journal of Rock*
804 *Mechanics and Mining Sciences & Geomechanics Abstracts* 2 (2), 245.
805 [https://doi.org/10.1016/0148-9062\(65\)90016-1](https://doi.org/10.1016/0148-9062(65)90016-1).
- 806